Modeling Distinct Osteosarcoma Subtypes *In Vivo* Using Cre:Lox and Lineage-Restricted Transgenic shRNA

Anthony J. Mutsaers, Alvin J.M. Ng, Emma K. Baker, Megan R. Russell, Alistair M. Chalk, Meaghan Wall, Brain J.J. Liddicoat, Patricia W.M. Ho, John L. Slavin, Ankita Goradia, T. John Martin, Louise E. Purton, Ross A. Dickins, Carl R. Walkley

PII: S8756-3282(13)00087-2
DOI: doi: 10.1016/j.bone.2013.02.016
Reference: BON 9960

To appear in: *Bone*

Received date: 3 January 2013
Revised date: 14 February 2013
Accepted date: 17 February 2013

Please cite this article as: Mutsaers Anthony J., Ng Alvin J.M., Baker Emma K., Russell Megan R., Chalk Alistair M., Wall Meaghan, Liddicoat Brain J.J., Ho Patricia W.M., Slavin John L., Goradia Ankita, Martin T. John, Purton Louise E., Dickins Ross A., Walkley Carl R., Modeling Distinct Osteosarcoma Subtypes *In Vivo* Using Cre:Lox and Lineage-Restricted Transgenic shRNA, *Bone* (2013), doi: 10.1016/j.bone.2013.02.016

Modeling Distinct Osteosarcoma Subtypes *In Vivo* Using Cre:Lox and Lineage-Restricted Transgenic shRNA.

Anthony J Mutsaers[1,6], Alvin JM Ng[1,2], Emma K Baker[1,2], Megan R Russell[1], Alistair M Chalk[1], Meaghan Wall[3], Brain JJ Liddicoat[1,2], Patricia WM Ho[1], John L Slavin[4], Ankita Goradia[1], T John Martin[1,2], Louise E Purton[1,2], Ross A Dickins[5] & Carl R Walkley[1,2*]

[1]St. Vincent's Institute of Medical Research, Fitzroy, Victoria, Australia;
[2]Department of Medicine, St. Vincent's Hospital, University of Melbourne, Fitzroy, Victoria, Australia;
[3]Victorian Cancer Cytogenetics Service, St. Vincent's Hospital, Fitzroy, Victoria, Australia;
[4]Department of Pathology, St Vincent's Hospital, Fitzroy, Victoria, Australia;
[5]Molecular Medicine Division, Walter and Eliza Hall Institute of Medical Research, Parkville, Victoria, Australia.
[6]Present Address: Ontario Veterinary College, University of Guelph, Guelph, Ontario, Canada.

*Correspondence should be addressed to:
Carl Walkley
St. Vincent's Institute
9 Princes St
Fitzroy, Victoria 3065
Australia
T: 61 3 9288 2480
Email: cwalkley@svi.edu.au

Keywords: osteosarcoma; p53; shRNA; osteoblastic subtype.

Abstract

Osteosarcoma is the most common primary cancer of bone and one that predominantly affects children and adolescents. Osteoblastic osteosarcoma represents the major subtype of this tumor, with approximately equal representation of fibroblastic and chondroblastic subtypes. We and others have previously described murine models of osteosarcoma based on osteoblast-restricted Cre:lox deletion of *Trp53 (p53)* and *Rb1 (Rb)*, resulting in a phenotype most similar to fibroblastic osteosarcoma in humans. We now report a model of the most prevalent form of human osteosarcoma, the osteoblastic subtype. In contrast to other osteosarcoma models that have used Cre:lox mediated gene deletion, this model was generated through shRNA-based knockdown of p53. As is the case with the human disease the shRNA tumors most frequently present in the long bones and preferentially disseminate to the lungs; features less consistently modeled using Cre:lox approaches. Our approach allowed direct comparison of the *in vivo* consequences of targeting the same genetic drivers using two different technologies, Cre:lox and shRNA. This demonstrated that the effects of Cre:lox and shRNA mediated knock-down are qualitatively different, at least in the context of osteosarcoma, and yielded distinct subtypes of osteosarcoma. Through the use of complementary genetic modification strategies we have established a model of the most common clinical subtype of osteosarcoma that was not previously represented and more fully recapitulated the clinical spectrum of this cancer.

1. Introduction

Osteosarcoma (OS) is the most common primary tumor of bone, occurring predominantly in the second decade of life. Conventional osteosarcoma presents as three major subtypes based on histological classifications: osteoblastic, fibroblastic and chondroblastic. Of the OS subtypes osteoblastic is the most common (~60%) with fibroblastic and chondroblastic being approximately equally represented [1]. Despite intensive research efforts, outcomes for patients with OS have not significantly improved in the last three decades [2]. Five year survival for patients with localized disease approaches 70% but falls to between 20-30% for patients with recurrent disease or metastasis at diagnosis [2]. Improving outcomes for these patients will require a concerted effort utilizing a number of approaches, of which accurate murine models form a key pillar [3]. In particular the ability to model and test interventions against highly penetrant and reproducible metastatic disease would be of significant advantage.

Murine models of OS generated over past decades have utilized many approaches including radiation exposure and carcinogens [4, 5]. The recent establishment of tractable genetically defined murine models based on the genetics of human disease offers a new means to understand the molecular genetics of OS and provide for further preclinical testing. Knowledge from the familial OS predisposition syndromes Li-Fraumeni syndrome and hereditary retinoblastoma has been applied to develop models that mirror human OS [6-8]. These models have used conditional Cre:lox alleles of *p53* (*Trp53,* Li-Fraumeni syndrome) and *Rb* (*Rb1,* hereditary retinoblastoma) and a range of osteoblastic lineage Cre transgenics. OS arising in these Cre:lox models shares cardinal features with human OS. The tumors resemble conventional human medullary OS, most closely approximating the fibroblastic/undifferentiated form [6, 7]. The development of OS models that encompass the spectrum of clinical OS subtypes (osteoblastic, chondroblastic and fibroblastic) would provide a broad pre-clinical platform to advance proposed therapies in a more precise manner [9].

Rapid improvements in the fidelity of murine models of human cancer have come about through the use of Cre:lox based approaches to elicit temporal and lineage specific gene modulation [7, 10, 11]. Recently developed transgenic, tetracycline (tet)-regulated shRNA based approaches have allowed for inhibition of endogenous gene expression *in vivo* [12, 13]. These have demonstrated efficacy in hematopoietic tumors but have not to date been reported in solid tumor models [13, 14]. A direct comparison of Cre:lox and shRNA approaches in modeling solid tumors is yet to be reported. One outstanding question is how comparable the effects of gene knockout are compared to gene knockdown on the tumor phenotype. The knockdown of a tumor suppressor which is highly mutated in human cancer, such as p53, may result in distinct selective pressures that are not apparent when genomic deletion is used.

Here we describe a new OS model that has utilised *in vivo* lineage restricted shRNA technology to bring about osteoblast specific knockdown of p53. We have also assessed the effects of concomitant deletion of *Rb*, known to potentiate OS formation in Cre:lox models but not itself act as an initiating event, with shRNA mediated suppression of p53. These mice develop OS, dependent on p53 loss of function, with near 100% penetrance but at longer latency than Cre:lox-based models targeting the same genetic drivers of OS. In contrast to previous models, tumors in this model more often develop in the long bone and are highly metastatic, features similar to human OS. Compared to Cre:lox tumors, which resemble human fibroblastic or undifferentiated OS, shRNA-driven tumors demonstrate a homogenous osteoblastic OS phenotype. As such, conditional deletion and shRNA mediated knockdown are distinctive *in vivo* tools and are highly complementary in efforts to establish a collection of murine models that reflect the diverse pathology of human solid tumors.

2. Materials and Methods

Detailed methods can be found in the supplemental section

2.1 Animals

p53.1224 transgenic animals were on a C57Bl6 background [13]; *pRb*$^{fl/fl}$ animals have been previously described and were on a C57Bl6 background [15]; *Osx*-Cre animals have been previously described and were on a C57Bl6 background [16]. Where mentioned the *Osx*-Cre *p53*$^{fl/fl}$*pRb*$^{fl/fl}$ line is the same as that previously described except the mice are from a 4 generation C57Bl6 background [7]. Balb/c nu/nu mice were used as recipients for transplant of primary tumor samples and OS cell lines. All experiments were approved by the AEC (St. Vincent's Hospital, Melbourne).

2.2 Kaplan-Meier Survival Analysis and statistical analysis

K-M survival plots were prepared using Prism software. Statistical analysis was done using Prism software using Mann-Whitney test and where indicated ANOVA with Bonferroni post-test correction.

2.3 MicroCT Imaging

Micro-computed tomography (μCT) analysis was performed according to standard procedures using Skyscan1076 (x-ray potential 50KVp, Kontich, Belgium) [17]. A full description is provided in the supplemental methods.

2.4 Microarray Sample Preparation and Analysis

Raw data files are available from the NCBI GEO browser (GSE38742). A full description is provided in the supplemental methods.

2.5 Flow Cytometry

Primary osteoblasts were isolated from crushed, digested femur/tibia/iliac crest bones. Hematopoietic cells were filtered out (40μm cell strainer) and the remaining bone was digested with collagenase as described [18]. OS cell lines were prepared from early passage (less than passage 5) cultures by trypsinisation. Antibodies are listed in supplemental methods. Flow cytometry was performed on a FACS LSRII Fortessa interfaced with CellQuest software, data was analyzed in FlowJo (TreeStar). Cell sorting was performed on a FACS Aria.

3. Results

3.1 Transgenic knockdown of endogenous gene expression in osteoblastic cells.

To establish the efficacy of transgenic short hairpin RNA (shRNA) in a lineage-restricted manner, we made use of transgenic mice harboring a microRNA-based shRNA targeting murine p53 driven by a tet-regulated TRE promoter [13]. This allele has been extensively characterized and validated to result in an efficient knock-down of both transcript and protein levels of p53 with no reported non specific effects [12, 19, 20]. These TRE-p53.1224 mice were crossed with *Osx*-Cre mice (Fig 1A-1B) [7]. The *Osx*-Cre transgene expresses a tetracycline transactivator (tTA) and GFP-Cre under the control of the *Osx* promoter that largely restricts expression to pre-osteoblasts. GFP identifies cells in which the tTA is transcriptionally active, driving expression of both the p53.1224 shRNA and GFP-Cre. We have not observed expression of GFP outside of the phenotypic osteoblastic lineage nor have we utilized the doxycyline regulatory capacity to modulate the activity of the tTA in these studies.

To assess knockdown of endogenous p53 we isolated primary osteoblastic cells from the *Osx*-Cre^{+}p53.1224^{+} or control animals and performed qPCR. The expression of GFP, indicative of active tTA which mediates expression of the p53.1224 shRNA, and the reduction of endogenous p53 levels were tightly related (Fig 1C, Supp Fig 1). We observed a greater than 90% reduction in the expression of the endogenous p53 transcript. This demonstrates effective, osteoblastic restricted p53 knockdown *in vivo*.

3.2 Highly penetrant osteosarcoma using shRNA transgenics.

In aiming to generate solid tumors we based our approach on our previous study that generated OS following *Osx*-Cre mediated deletion of $p53^{fl/fl}$ and $Rb^{fl/fl}$ alleles in osteoblastic cells [7]. *Osx*-Cre p53.1224 mice were crossed with $pRb^{fl/fl}$ mice, as this potentiates tumor formation in a p53 dependent manner [7]. As previously reported, loss of *Rb* alone does not result in OS. We observed tumor formation in the shRNA mice (referred as shRNA OS) with

a mean latency of 409 days, significantly longer than using Cre:lox alleles (referred to as Cre:lox OS) where median tumor latency was 177 days (Figure 1D, Supp Table 1).

Differences in the presentation of OS between the two approaches were readily apparent. Firstly, a greater proportion of tumors were found on the lower long bones using shRNA (60% shRNA OS vs 29% Cre:lox OS) accompanied by a reduction in OS formation on the mandible/head (Supp Table 1). Secondly, 70% of shRNA mice had metastatic disease at autopsy compared to 29% of Cre:lox animals. Metastatic dissemination to the lung and liver was common, mimicking the hematogenous pattern of spread observed in patients with OS (Supp Table 1). The anatomical distribution combined with the slower proliferation of the shRNA cells compared to the Cre:lox OS cells may substantially improve the rates of metastatic dissemination as animals survive for a significantly longer period in the shRNA model than the Cre:lox model where tumours on the head necessitate early euthanasia (Supp Figure 7). We have not observed non osteoblastic lineage sarcomas or hibernoma (brown fat tumor) formation in the shRNA model as has been reported in the Cre:lox mice [6, 7]. Consistent with our previous data, homozygous deletion of *Rb* accelerated tumor formation in the Cre:lox model (Supp Fig 2A). Interestingly, concomitant deletion of *Rb* in the shRNA model did not significantly accelerate tumor formation albeit in a small cohort size (Supp Fig 2B). However, it is possible subset analysis per genotype in small cohorts lacked the statistical power to identify subtle effects of concomitant *Rb* deletion in the shRNA OS model.

It was appreciable that shRNA mediated knockdown was functionally distinct from deletion using Cre:lox based on the survival amongst $p53^{fl/fl}$, $p53^{fl/+}$ and p53.1224 cohorts that all had $Rb^{+/+}$ alleles (Supp Fig 2F). While the knockdown of p53 reduced gene dosage of p53 by a much greater degree than that in the somatic heterozygous state, the shRNA median survival was considerably longer than that of $p53^{fl/+}$ animals. Thus, the shRNA mediated knockdown of p53 was functionally distinct from gross deletion of p53 using Cre:lox methods. Collectively these results demonstrate that loss of p53 is the driving genetic lesion leading to initiation of OS irrespective of the means used to reduce p53 expression.

3.3 A model of the osteoblastic subtype of osteosarcoma

A most striking difference between OS arising in the p53 knockdown shRNA model compared with the p53 deficient Cre:lox model was the degree of tumor mineralization. Cre:lox OS is characterized by predominant areas of fibroblastic (undifferentiated) morphology accompanied by intermittent areas of mineralized osteoid (Figure 1E) confirmed by von Kossa staining (Figure 1F). In contrast, the shRNA OS almost invariably had a uniform heavily mineralized osteoblastic (well differentiated) OS appearance in both primary and metastatic sites (Figure 1F-G). High degrees of mineralization were apparent both in primary and metastatic lesions, independent of site (Figure 1F). The shRNA OS tumors closely resemble osteoblastic OS, the most common subtype in humans.

The mineralized nature of the shRNA OS made them readily detectable using micro-computed tomography (μCT). The increased mineralization and radiographic density of the shRNA OS was clearly discernible compared to the Cre:lox (Figure 2A-B). The ability to detect OS in the shRNA model made it possible to identify sites of OS that were not otherwise apparent clinically or at autopsy, such as occult disease within the spinal column (white arrow, Figure 2C)). Mineralization of metastatic lesions, including in the lung, suggested this was a property intrinsic to the shRNA OS lesions (Figure 2D). Consistent with this, when placed as xenografts, cell lines from the shRNA OS also developed a high degree of mineralization (data not shown). One advantage of the ease of detection of small shRNA OS lesions by μCT was the ability to longitudinally monitor OS development. For example, we detected a small lesion in the fibula and monitored its *in vivo* progression by serial imaging (Figure 2E).

3.4 Differentiation marker analysis confirm differentiated nature of shRNA OS

To confirm the histological findings, qPCR on whole tumors and cell surface profiling of primary OS cell cultures (< passage 5) was performed. Cell cultures were readily

established from both models by mechanical dissociation and plating. Cultures from shRNA tumors proliferated significantly more slowly than those obtained from Cre:lox tumors (Supp Fig 7). A range of markers representing stages of osteoblast differentiation was assessed (Figure 2F). shRNA OS had the gene expression pattern of a more differentiated cell type than Cre:lox OS (Figure 2G). Under *in vitro* differentiation conditions the shRNA OS cell cultures more rapidly mineralised compared to Cre:lox OS, in keeping with a mature osteoblast (Supp Fig 3). Furthermore, shRNA OS failed to become adipogenic under inductive conditions, whereas Cre:lox tumors retain adipogenic potential consistent with a pre-osteoblast (Supp Fig 3). Also in keeping with a more differentiated state, shRNA OS animals had higher serum alkaline phosphatase levels than their Cre:lox counterparts (Figure 2H). Therefore the shRNA OS represents a cell population that is osteoblast restricted and is beyond the stage at which it is able to undergo differentiation along the alternate adipogenic lineage.

We next sought to determine the nature and extent of the response of the tumours to stimulation of the parathyroid hormone receptor (PTHR1), prostaglandin receptors and β-adrenergic receptors, all critical regulators of osteoblast differentiation. shRNA OS expressed higher levels of the PTHR1 than Cre:lox OS. To functionally assess this we compared the cyclic AMP (cAMP) response of Cre:lox and shRNA OS cell lines to PTH(1-34), prostaglandin E2 (PGE_2) and isoproterenol (Iso, Figure 2H). Cells from both tumors displayed PTH responsiveness, however Cre:lox OS have a ratio of PTH:Iso response of less than 1 consistent with pre-osteoblasts. In contrast, shRNA OS have a PTH:Iso of greater than 2 which is reflective of their mature osteoblastic phenotype and gene expression profile (Figure 2I, Supp Fig 4). PGE_2 response was largely comparable between the models. Collectively these data demonstrate that the fibroblastic and osteoblastic OS subtype models are qualitatively distinct in regards to their differentiation stage.

Early passage cell lines (< passage 5) were assessed for surface expression of Sca-1 and CD51 (Integrin αV) [7]. Pre-osteoblastic cells have a phenotype that is hematopoietic

(CD45) and endothelial (CD31) marker negative and Sca-1^{+}CD51^{+}. As cells mature they become Sca-$1^{lo/-}$CD$51^{lo/+}$ osteoblasts (Figure 3A). Consistent with our previous analysis Cre:lox OS lines are Sca-1^{+}CD51^{+}, corresponding to their assignment as pre-osteoblasts [7] (Figure 3A). The *Osx*-Cre transgene (GFP signal) can be detected in a significant proportion of the Sca-1^{+} population serving as an endogenous transcriptional reporter of the pre-osteoblastic state (Figure 3B). Further analysis using the recently described marker PDGFRα (CD140a) demonstrated that the Cre:lox OS cells are predominantly Sca-1^{+}CD51^{+}PDGFRα^{+} (Figure 3C) [21]. The shRNA OS and metastatic lines were predominantly Sca-$1^{lo/-}$CD$51^{lo/+}$, the surface expression pattern of mature osteoblasts. The cells were essentially negative for both the *Osx*-Cre transgene (GFP) and PDGFRα. Thus the surface marker profile, qPCR and histological presentation all demonstrated that the OS arising through use of shRNA knock-down of p53 is an osteoblastic OS distinct from the less-differentiated, pre-osteoblastic OS subtype generated using Cre:lox mediated deletion of p53.

3.5 Disabling of the endogenous p53 pathway in the absence of hairpin expression

One attractive feature of the transgenic shRNA models is the potential for reversible loss of function [12, 13]. Having demonstrated that p53 knockdown led to OS development (Figure 1), we reasoned that reactivation of p53 in established OS would allow assessment of the tumor dependence on p53 suppression. In principle, the *Osx*-Cre strategy should result in co-expression of GFP and p53 shRNA during OS development as both are controlled by tTA-dependent TRE promoters. However, we were surprised to find that shRNA tumors contained very low to negligible levels of GFP, even in the absence of doxycycline (Figure 3B). This suggested that either the *Osx*-Cre promoter was not active in the tumors, that p53 shRNA expression had somehow been uncoupled from GFP reporter expression during OS development, or that the shRNA-driven OS cells had evolved to become independent of p53 knockdown. We have previously observed that there are only low levels of GFP, reflective of expression of the *Osx*-Cre transgene and tTA, in adult mice and OS cells isolated from

Cre:lox tumors. This is most consistent with the transgene not being robustly expressed throughout osteoblast development but rather in a window of development coinciding with pre-osteoblastic cells. Therefore we assessed the p53 response in primary cell cultures derived from shRNA OS to ascertain the status of the p53 pathway in the tumors.

In Cre:lox OS, which is p53 deficient, there are barely detectable levels of endogenous p53 expression in early passage cell lines, likely arising from minor hematopoietic contaminants (<1% CD45+ve cells; Figure 4A). There was a 2-log reduction in endogenous p53 expression in shRNA OS lines compared to control (<1% CD45+ve cells; Figure 4A). However, compared to Cre:lox OS cell lines, shRNA OS lines have a 2-log increase in p53 transcript levels. To assess if the p53 pathway was functional the induction of classical p53 target genes $p21^{Cip1}$ and Noxa in response to doxorubicin was determined [22]. The control primary osteoblasts displayed a robust induction of both $p21^{Cip1}$ and *Noxa* in response to doxorubicin (Figure 4B), whereas the p53 deficient Cre:lox OS cells can not activate a p53 response (Figure 4B). The shRNA OS cell lines failed to induce expression of either $p21^{Cip1}$ or *Noxa*, displaying a response similar to $p53^{-/-}$ OS cells indicating that the endogenous p53 pathway had become inactivated (Figure 4B). To ascertain the status of endogenous p53 we performed direct sequencing of exons 4-9 using Sanger sequencing and exome capture sequencing and did not find somatic mutations in the p53 exons (data not shown). Analysis of the gene expression data revealed no difference in the expression of *Mdm1*, *Mdm2* or *Mdm4* between Cre:lox and shRNA OS tumors, indicating that amplification of one of these p53 regulators was not likely a means of inactivation of the p53 response (data not shown). Over-expression of Twist1 was recently reported to be a common event in sarcoma and resulted in the inactivation of wild-type p53 function [23]. We found a 2-fold elevation in *Twist* mRNA expression between Cre:lox OS and shRNA OS cell lines. Knock-down of Twist1 in shRNA OS cell lines was unable to restore p53 induced gene induction following doxorubicin treatment (data not shown).

We finally assessed if the endogenous p53 allele had undergone methylation-induced silencing [24]. Doxorubicin treatment of the control Kusa4b10 osteoblastic cell line elicited a

strong induction of *Noxa* expression, which was further enhanced by treatment with the demethylating agent 5-Aza-2'-deoxycytidine (5-AzadC; Figure 4C). Treatment of shRNA OS cells with 5-AzadC did not affect the expression of the endogenous p53 transcript (Figure 4C). Furthermore, treatment with 5-AzadC and doxorubicin failed to induce the expression of *Noxa*, demonstrating that the p53 pathway in shRNA OS is not functional (Figure 4C). These studies demonstrate that the shRNA OS cells have evolved an inactive p53 pathway, thus becoming independent of the continued requirement for the shRNA activity.

3.6 Karyotypic complexity with recurrent changes

A hallmark of human OS is karyotypic complexity in the absence of recurrent translocations [25]. We assessed early passage OS cultures derived from the shRNA tumors (Figure 5A). All shRNA OS had clonal cytogenetic abnormalities and demonstrated karyotypic complexity. Multiple clonal numerical abnormalities were present in all cases and clonal structural abnormalities detectable at the resolution of metaphase cytogenetics were present in 4/6 tumors. The most frequent changes were recurrent gains of chromosomes 14 and 15 and loss of chromosome 3, 7 and 12, all of which were present in at least 50% of cases. Most striking was recurrent loss of chromosome 7 (n=6/6) (Figure 5B). A reassessment of data from the Cre:lox OS also revealed frequent loss of chromosome 7 [7], suggesting that this may be a common mechanism to generate OS. Chromosomes 6, 8 and 15 were the chromosomes most commonly involved in inter-chromosomal rearrangement (Figure 5C). Chromosome 15 demonstrated a very high rate of collective abnormalities, including copy number gain or structural rearrangement (Figure 5C). As is seen with human OS none of the translocations were recurrent. Therefore, independent of the means used to disrupt p53, cells proceed via a common pathway involving loss of chromosome 7 and copy number increase/rearrangement of chromosome 15 during OS development. The non-random, recurrent nature of the abnormalities suggests that shRNA OS tumors share programmed major pathways of tumor initiation and progression.

3.7 Gene expression profiles and comparison to human

To determine if the distinct histology of the fibroblastic and osteoblastic OS models was associated with a specific gene expression pattern we conducted micro-array analysis. When assessed at a level of 2 fold or greater change in gene expression and a statistical significance level of $P<0.05$, less than 3% of expressed (273 of 9361) genes were differentially expressed between Cre:lox and shRNA OS respectively (Figure 6A). The shRNA OS had increased expression of genes associated with mature osteoblasts such as *osteocalcin* and *DMP1* concordant with our qPCR analysis. Interestingly, there was evidence of differential expression of components of the Wnt pathway between the models. This is consistent with the known roles for this pathway in the regulation of osteoblast differentiation and its altered expression in human OS [26, 27]. There were also changes in the expression of different matrix /cell surface and signaling transcripts.

We next assessed co-ordinate changes in gene expression signatures using the gene set enrichment analysis (GSEA) approach and Ingenuity Pathway Analysis (IPA) [28]. The most significantly enriched signature using GSEA in Cre:lox OS was a gene set associated with acute deletion of the *Rb* gene (Figure 6B). This was unexpected as both groups contained the same *Rb* allele distribution amongst the samples (three $Rb^{fl/+}$ and one $Rb^{+/+}$) although consistent with the lack of disease acceleration seen in the shRNA model by concomitant deletion of Rb. The other major pathway upregulated in Cre:lox tumors was a gene set associated with hypoxia (Figure 6B). The maintenance of a hypoxic state is known to restrain the differentiation of osteoblastic cells and was also observed using IPA (Figure 6C) [29]. IPA analysis also revealed activation of TNF and TGFβ transcriptional programs in Cre:lox OS (Figure 6C). In the shRNA OS there was enrichment of gene sets associated with chromosomal aberrations in a range of human cancers and with cell-cell junctions and adhesion (Supp Fig 5). Collectively these analyses suggest that there are distinctive gene expression signatures associated with each OS subtype that may contribute to the differentiation stage of the tumors.

Next, we compared the shRNA and Cre:lox OS to human sarcomas and other defined murine sarcoma models using the metagene projection methodology [7, 30]. The metagene training set for a subset of human sarcomas was obtained from a dataset of human mesenchymal derived tumors (Figure 6D) [31]. We validated the metagene classifiers through addition of test sets obtained from independently derived human sarcoma profiles [32, 33]. This demonstrated that the metagene approach performed as a robust classifier of sarcoma. The Cre:lox and shRNA OS samples were then applied as test sets, resulting in a clear association of the current murine OS models with the human OS samples (F7 metagene classifier; Figure 6D). Murine OS we have previously described (mOS (Cre:lox)) and those derived independently from *p53*$^{+/-}$ animals also align with the human OS and Cre:lox and shRNA OS models [34]. Comparison to other murine sarcoma models demonstrated that OS represents a distinct entity from other mesenchymal derived tumors such as genetically engineered synovial sarcoma models [32, 35, 36]. One interesting finding is that irrespective of the means used to modulate p53 in murine models of OS the resulting tumors share a gene expression signature of human OS. These analyses demonstrate the shRNA and Cre:lox models of OS generated are faithful representations of human OS.

4. Discussion

Collectively the data demonstrate that lineage restricted shRNA against p53 is able to efficiently induce solid tumors, in this iteration osteosarcoma. We propose a model whereby use of Cre:lox alleles of p53 results in acute effect on differentiation and immortalisation of a pre-osteoblastic cell, ultimately leading to a fibroblastic OS (Figure 7B). This is consistent with previous reports where loss of p53 leads to an increased expression of both *Runx2* and *Osterix* and an increase in proliferation [37]. The knockdown of p53 using the shRNA approach would be predicted to result in a less sudden arrest in cell maturation and differentiation, allowing osteoblast differentiation to proceed further prior to immortalization (Figure 7C). This would account for the development of a more differentiated OS and an osteoblastic phenotype. The experimental outcome raises the possibility that OS can arise from different stages within the osteoblastic lineage and that the cellular maturation stage of origin dictates the tumor presentation. Such a model would be consistent with a cell-of-origin model of OS, where the different subtypes arise as a result of mutation within the cells of a distinct differentiation stage within the osteoblast lineage rather than from mutations in mesenchymal stem cells [38].

The use of shRNA for tumor modeling has been most widely reported in the hematopoietic system, where high levels of expression can be enforced by retroviral infection approaches and coupling of the tTA/rtTA to the tumor initiating oncogene [14]. Recently several groups have reported application of shRNA to solid tumor modeling with varying efficiency. Inducible knockdown of PDK1 in the whole animal using a *Rosa26* knock-in approach was found to have no effect on tumourigenesis dependent on PTEN deficiency [39]. Knockdown of GATA4 in the whole animal resulted in a range of phenotypes and a 10% incidence of ovarian teratoma [40]. Our study is distinct from these in that we have demonstrated the efficacy of lineage-restricted knockdown with a high incidence of tumor initiation driven by reductions in p53 levels.

A compelling finding from these studies is that inactivation of the p53 pathway is the driving lesion required to generate experimental OS. The concurrent deletion of *Rb* can

accelerate OS formation in the absence of *p53* but cannot function as an initiating event itself. This is consistent with a range of other models utilizing either *p53* conditional alleles and different menenchymal/osteoblastic Cre lines or transgenic models over-expressing T antigen [5, 8]. It is apparent that the p53.1224 shRNA results in a strong pressure to inactivate the endogenous p53 pathway. This observation may become important with the increase in efforts to silence tumor suppressors using shRNA. Whilst we have been unable to define the nature of the disruption of the p53 pathway, the shRNA OS cells are deficient in the p53 response following exposure to chemotherapy. This is evident from the functional tests and also the microarray comparisons where the core genetic signatures of OS derived by shRNA are largely indistinguishable from that of p53 deficient OS. Our results demonstrated that, at least in this example, the effects of complete loss and knock-down of gene expression are qualitatively different and result in distinctive pathology, similar to that described for *Pten* [41, 42]. We had previously observed that tumors arising in the Cre:lox model from $p53^{fl/+}$ animals evolved with loss of heterozygosity of the retained p53 allele [7]. This result together with the results from the shRNA model would strongly imply that near complete inactivation of the p53 pathway is absolutely required for OS.

Karyotypic analysis of the shRNA OS identified clonal, chromosomal alterations arising during the process of evolution of OS that are recurrent. These included loss of chromosome 7 and a gain or rearrangement of chromosome 15. Chromosome 7 copy number was reduced in both shRNA and Cre:lox OS. Where cells are tetraploid, chromosome 7 is present at a reduced, but never completely absent, copy number. Mouse chromosome 7 is syntenic to regions of human chromosomes 10, 11, 15, 16 and 19 (Ensembl). Of these, syntenic sections of 10, 11 and 16 are also lost in cases of human OS [43, 44]. Candidate genes of interest on chromosome 7 include the Wnt pathway members DKK3 [45] and Wnt11 [46] which have roles in promoting osteoblast maturation. Chromosome 15 in mouse shows homology with human chromosome 5, 8, 12 and 22. All but the region of 22 show amplification of conserved regions in human OS, and human *MYC* is found on chromosome 8 [43]. The most compelling candidate on mouse chromosome 15 is amplification of *c-Myc*.

Ectopic expression of c-Myc was demonstrated to induce OS *in vivo* and was able to contribute to transformation of mesenchymal progenitors that gave rise to OS on transplantation [47, 48]. Interestingly in both of these cases there was a significant contribution from the inactivation of the "Rb-pathway", as either a co-operative mutation or in modifying the response to Myc reactivation. The region containing *c-Myc* was also frequently amplified in OS arising in $p53^{+/-}$ animals [35]. Another gene of interest, linked to the same genomic region as c-Myc, is osteoprotegerin (OPG). OPG is secreted by osteoblasts and acts as a decoy receptor to inhibit bone resorption and is produced by human OS lines [49, 50]. These analyses suggest that pre-osteoblasts/osteoblasts undergo a recurrent path that involves inactivation of both the p53 and Rb pathways, a gain of *Myc* (Chr 15 gain/rearrangement) and the reduction in gene dosage of chromosome 7.

Through use of a distinct genetic modification technology for perturbing p53 function in osteoblasts we have revealed a new model of a tumor subtype. The contribution of the tTA line cannot be understated. It may be that a more highly active tTA in the osteoblast lineage would result in an disease more comparable to that from Cre:lox approaches. The *Osx* driven tTA may lend itself to a subtlety of phenotype that is permissive for the generation of the osteoblastic OS. Modeling solid tumors using the approach described may be advantageous in recapitulating the selective pressure placed on critical pathways, such as p53, in human cancers. These results also demonstrate that, at least in the case of p53, genetic deletion using Cre:lox technology and gene knock-down using shRNA are not directly comparable and can elicit distinct pressures during tumor evolution *in vivo*. As such, the process of initiation and maintenance may more closely resemble the process in human cells, also resulting in an extended latency and increase in metastatic disease.

5. Conclusion

The variation in any human cancer can only be adequately captured experimentally through the use of more than one murine model. We and others have previously described an OS model where mice present with a phenotype most similar to fibroblastic/undifferentiated OS [6, 7]. We now report a highly penetrant model of osteoblastic OS with a high frequency of metastatic dissemination. The development of this new line provides a valuable new experimental tool and establishes a model of the most common form of clinically managed OS [9]. Through a cross species comparison we demonstrate that both Cre:lox and shRNA OS models are faithful recapitulations of human OS validating these as useful for further pre-clinical application. shRNA OS is an osteoblastic subtype, in contrast to a predominantly fibroblastic generated using Cre:lox based deletion of p53.

Acknowledgements:

We thank T Jacks and A McMahon for providing *pRb*$^{fl/fl}$ and *Osx*-Cre lines respectively; SVH BioResources Centre; N Sanders for FACS sorting; M Walia for proliferation curves; I Poulton for technical assistance; S Orkin, N Walsh, V Sankaran and J Heierhorst for comments and discussion.

This work was supported by grants from the National Health and Medical Research Council of Australia (NHMRC; to C.W. and C.W./T.J.M.); AACR-Aflac, Inc Career Development Award for Pediatric Cancer Research (C.W.); NHMRC Career Development Award (C.W.); NHMRC Senior Research Fellowship (L.P.); Victorian Cancer Agency Early Career Seed Grant (C.W); Victorian Cancer Agency Clinical Research Fellowship (M.W.); Cancer Therapeutics CRC (CTx) postgraduate scholarship (A.N.); Cure Cancer Australia Fellowship (E.B.); in part by the Victorian State Government Operational Infrastructure Support Program (to St. Vincent's Institute). C.W. is the Philip Desbrow Senior Research Fellow of the Leukaemia Foundation.

The authors declare no competing financial interest.

References

[1] Bacci G, Longhi A, Fagioli F, Briccoli A, Versari M, Picci P. Adjuvant and neoadjuvant chemotherapy for osteosarcoma of the extremities: 27 year experience at Rizzoli Institute, Italy. Eur J Cancer 2005;41: 2836-45.
[2] Janeway KA, Barkauskas DA, Krailo MD, Meyers PA, Schwartz CL, Ebb DH, Seibel NL, Grier HE, Gorlick R, Marina N. Outcome for adolescent and young adult patients with osteosarcoma: a report from the Children's Oncology Group. Cancer 2012;118: 4597-605.
[3] Ng AJ, Mutsaers AJ, Baker EK, Walkley CR. Genetically engineered mouse models and human osteosarcoma. Clin Sarcoma Res 2012;2: 19.
[4] Martin TJ, Ingleton PM, Underwood JC, Michelangeli VP, Hunt NH, Melick RA. Parathyroid hormone-responsive adenylate cyclase in induced transplantable osteogenic rat sarcoma. Nature 1976;260: 436-8.
[5] Molyneux SD, Di Grappa MA, Beristain AG, McKee TD, Wai DH, Paderova J, Kashyap M, Hu P, Maiuri T, Narala SR, Stambolic V, Squire J, Penninger J, Sanchez O, Triche TJ, Wood GA, Kirschner LS, Khokha R. Prkar1a is an osteosarcoma tumor suppressor that defines a molecular subclass in mice. J Clin Invest 2010;120: 3310-25.
[6] Berman SD, Calo E, Landman AS, Danielian PS, Miller ES, West JC, Fonhoue BD, Caron A, Bronson R, Bouxsein ML, Mukherjee S, Lees JA. Metastatic osteosarcoma induced by inactivation of Rb and p53 in the osteoblast lineage. Proc Natl Acad Sci U S A 2008;105: 11851-6.
[7] Walkley CR, Qudsi R, Sankaran VG, Perry JA, Gostissa M, Roth SI, Rodda SJ, Snay E, Dunning P, Fahey FH, Alt FW, McMahon AP, Orkin SH. Conditional mouse osteosarcoma, dependent on p53 loss and potentiated by loss of Rb, mimics the human disease. Genes Dev 2008;22: 1662-1676.
[8] Lin PP, Pandey MK, Jin F, Raymond AK, Akiyama H, Lozano G. Targeted mutation of p53 and Rb in mesenchymal cells of the limb bud produces sarcomas in mice. Carcinogenesis 2009;30: 1789-95.
[9] Sellers WR. A blueprint for advancing genetics-based cancer therapy. Cell 2011;147: 26-31.
[10] Frese KK, Tuveson DA. Maximizing mouse cancer models. Nat Rev Cancer 2007;7: 654-8.
[11] Li Z, Tognon CE, Godinho FJ, Yasaitis L, Hock H, Herschkowitz JI, Lannon CL, Cho E, Kim SJ, Bronson RT, Perou CM, Sorensen PH, Orkin SH. ETV6-NTRK3 fusion oncogene initiates breast cancer from committed mammary progenitors via activation of AP1 complex. Cancer Cell 2007;12: 542-58.
[12] Premsrirut PK, Dow LE, Kim SY, Camiolo M, Malone CD, Miething C, Scuoppo C, Zuber J, Dickins RA, Kogan SC, Shroyer KR, Sordella R, Hannon GJ, Lowe SW. A rapid and scalable system for studying gene function in mice using conditional RNA interference. Cell 2011;145: 145-58.
[13] Dickins RA, McJunkin K, Hernando E, Premsrirut PK, Krizhanovsky V, Burgess DJ, Kim SY, Cordon-Cardo C, Zender L, Hannon GJ, Lowe SW. Tissue-specific and reversible RNA interference in transgenic mice. Nat Genet 2007;39: 914-21.
[14] Zuber J, McJunkin K, Fellmann C, Dow LE, Taylor MJ, Hannon GJ, Lowe SW. Toolkit for evaluating genes required for proliferation and survival using tetracycline-regulated RNAi. Nat Biotechnol 2011;29: 79-83.
[15] MacPherson D, Sage J, Crowley D, Trumpp A, Bronson RT, Jacks T. Conditional mutation of Rb causes cell cycle defects without apoptosis in the central nervous system. Mol Cell Biol l2003;23: 1044-53.
[16] Rodda SJ, McMahon AP. Distinct roles for Hedgehog and canonical Wnt signaling in specification, differentiation and maintenance of osteoblast progenitors. Development 2006;133: 3231-44.
[17] Bouxsein ML, Boyd SK, Christiansen BA, Guldberg RE, Jepsen KJ, Muller R. Guidelines for assessment of bone microstructure in rodents using micro-computed tomography. J Bone Miner Res 2010;25: 1468-86.

[18] Singbrant S, Russell MR, Jovic T, Liddicoat B, Izon DJ, Purton LE, Sims NA, Martin TJ, Sankaran VG, Walkley CR. Erythropoietin couples erythropoiesis, B-lymphopoiesis, and bone homeostasis within the bone marrow microenvironment. Blood 2011;117: 5631-42.
[19] Krizhanovsky V, Yon M, Dickins RA, Hearn S, Simon J, Miething C, Yee H, Zender L, Lowe SW. Senescence of activated stellate cells limits liver fibrosis. Cell 2008;134: 657-67.
[20] Xue W, Zender L, Miething C, Dickins RA, Hernando E, Krizhanovsky V, Cordon-Cardo C, Lowe SW. Senescence and tumour clearance is triggered by p53 restoration in murine liver carcinomas. Nature 2007;445: 656-60.
[21] Morikawa S, Mabuchi Y, Kubota Y, Nagai Y, Niibe K, Hiratsu E, Suzuki S, Miyauchi-Hara C, Nagoshi N, Sunabori T, Shimmura S, Miyawaki A, Nakagawa T, Suda T, Okano H, Matsuzaki Y. Prospective identification, isolation, and systemic transplantation of multipotent mesenchymal stem cells in murine bone marrow. J Exp Med 2009;206: 2483-96.
[22] Brady CA, Jiang D, Mello SS, Johnson TM, Jarvis LA, Kozak MM, Kenzelmann Broz D, Basak S, Park EJ, McLaughlin ME, Karnezis AN, Attardi LD. Distinct p53 transcriptional programs dictate acute DNA-damage responses and tumor suppression. Cell 2011;145: 571-83.
[23] Piccinin S, Tonin E, Sessa S, Demontis S, Rossi S, Pecciarini L, Zanatta L, Pivetta F, Grizzo A, Sonego M, Rosano C, Dei Tos AP, Doglioni C, Maestro R. A "Twist box" Code of p53 Inactivation: Twist box:p53 Interaction Promotes p53 Degradation. Cancer Cell 2012;22: 404-15.
[24] Schroeder M, Mass MJ. CpG methylation inactivates the transcriptional activity of the promoter of the human p53 tumor suppressor gene. Biochem Biophys Res Commun 1997;235: 403-6.
[25] Taylor BS, Barretina J, Maki RG, Antonescu CR, Singer S, Ladanyi M. Advances in sarcoma genomics and new therapeutic targets. Nat Rev Cancer 2011;11: 541-57.
[26] Monroe DG, McGee-Lawrence ME, Oursler MJ, Westendorf JJ. Update on Wnt signaling in bone cell biology and bone disease. Gene 2012;492: 1-18.
[27] Cleton-Jansen AM, Anninga JK, Briaire-de Bruijn IH, Romeo S, Oosting J, Egeler RM, Gelderblom H, Taminiau AH, Hogendoorn PC. Profiling of high-grade central osteosarcoma and its putative progenitor cells identifies tumourigenic pathways. Br J Cancer 2009;101: 1909-18.
[28] Mootha VK, Lindgren CM, Eriksson KF, Subramanian A, Sihag S, Lehar J, Puigserver P, Carlsson E, Ridderstrale M, Laurila E, Houstis N, Daly MJ, Patterson N, Mesirov JP, Golub TR, Tamayo P, Spiegelman B, Lander ES, Hirschhorn JN, Altshuler D, Groop LC. PGC-1alpha-responsive genes involved in oxidative phosphorylation are coordinately downregulated in human diabetes. Nat Genet 2003;34: 267-73.
[29] Maes C, Carmeliet G, Schipani E. Hypoxia-driven pathways in bone development, regeneration and disease. Nat Rev Rheumatol 2012;8: 358-66.
[30] Tamayo P, Scanfeld D, Ebert BL, Gillette MA, Roberts CW, Mesirov JP. Metagene projection for cross-platform, cross-species characterization of global transcriptional states. Proc Natl Acad Sci U S A 2007;104: 5959-64.
[31] Henderson SR, Guiliano D, Presneau N, McLean S, Frow R, Vujovic S, Anderson J, Sebire N, Whelan J, Athanasou N, Flanagan AM, Boshoff C. A molecular map of mesenchymal tumors. Genome Biol 2005;6: R76.
[32] Rubin BP, Nishijo K, Chen HI, Yi X, Schuetze DP, Pal R, Prajapati SI, Abraham J, Arenkiel BR, Chen QR, Davis S, McCleish AT, Capecchi MR, Michalek JE, Zarzabal LA, Khan J, Yu Z, Parham DM, Barr FG, Meltzer PS, Chen Y, Keller C. Evidence for an unanticipated relationship between undifferentiated pleomorphic sarcoma and embryonal rhabdomyosarcoma. Cancer Cell 2011;19: 177-91.
[33] Nakayama R, Nemoto T, Takahashi H, Ohta T, Kawai A, Seki K, Yoshida T, Toyama Y, Ichikawa H, Hasegawa T. Gene expression analysis of soft tissue sarcomas: characterization and reclassification of malignant fibrous histiocytoma. Mod Pathol 2007;20: 749-59.

[34] Engin F, Bertin T, Ma O, Jiang MM, Wang L, Sutton RE, Donehower LA, Lee B. Notch signaling contributes to the pathogenesis of human osteosarcomas. Hum Mol Genet 2009;18: 1464-70.
[35] Ma O, Cai WW, Zender L, Dayaram T, Shen J, Herron AJ, Lowe SW, Man TK, Lau CC, Donehower LA. MMP13, Birc2 (cIAP1), and Birc3 (cIAP2), amplified on chromosome 9, collaborate with p53 deficiency in mouse osteosarcoma progression. Cancer Res 2009;69: 2559-67.
[36] Haldar M, Hancock JD, Coffin CM, Lessnick SL, Capecchi MR. A conditional mouse model of synovial sarcoma: insights into a myogenic origin. Cancer Cell 2007;11: 375-88.
[37] Wang X, Kua HY, Hu Y, Guo K, Zeng Q, Wu Q, Ng HH, Karsenty G, de Crombrugghe B, Yeh J, Li B. p53 functions as a negative regulator of osteoblastogenesis, osteoblast-dependent osteoclastogenesis, and bone remodeling. J Cell Biol 2006;172: 115-25.
[38] Visvader JE. Cells of origin in cancer. Nature 2011;469: 314-22.
[39] Ellwood-Yen K, Keilhack H, Kunii K, Dolinski B, Connor Y, Hu K, Nagashima K, O'Hare E, Erkul Y, Di Bacco A, Gargano D, Shomer NH, Angagaw M, Leccese E, Andrade P, Hurd M, Shin MK, Vogt TF, Northrup A, Bobkova EV, Kasibhatla S, Bronson RT, Scott ML, Draetta G, Richon V, Kohl N, Blume-Jensen P, Andersen JN, Kraus M. PDK1 attenuation fails to prevent tumor formation in PTEN-deficient transgenic mouse models. Cancer Res 2011;71: 3052-65.
[40] Thurisch B, Liang SY, Sarioglu N, Schomburg L, Bungert J, Dame C. Transgenic mice expressing small interfering RNA against Gata4 point to a crucial role of Gata4 in the heart and gonads. J Mol Endocrinol 2009;43: 157-69.
[41] Alimonti A, Carracedo A, Clohessy JG, Trotman LC, Nardella C, Egia A, Salmena L, Sampieri K, Haveman WJ, Brogi E, Richardson AL, Zhang J, Pandolfi PP. Subtle variations in Pten dose determine cancer susceptibility. Nat Genet 2010;42: 454-8.
[42] Carracedo A, Alimonti A, Pandolfi PP. PTEN level in tumor suppression: how much is too little? Cancer Res 2011;71: 629-33.
[43] Bayani J, Zielenska M, Pandita A, Al-Romaih K, Karaskova J, Harrison K, Bridge JA, Sorensen P, Thorner P, Squire JA. Spectral karyotyping identifies recurrent complex rearrangements of chromosomes 8, 17, and 20 in osteosarcomas. Genes Chromosomes Cancer 2003;36: 7-16.
[44] Kuijjer ML, Rydbeck H, Kresse SH, Buddingh EP, Lid AB, Roelofs H, Burger H, Myklebost O, Hogendoorn PC, Meza-Zepeda LA, Cleton-Jansen AM. Identification of osteosarcoma driver genes by integrative analysis of copy number and gene expression data. Genes Chromosomes Cancer 2012;51: 696-706.
[45] Daino K, Ugolin N, Altmeyer-Morel S, Guilly MN, Chevillard S. Gene expression profiling of alpha-radiation-induced rat osteosarcomas: identification of dysregulated genes involved in radiation-induced tumorigenesis of bone. Int J Cancer 2009;125: 612-20.
[46] Friedman MS, Oyserman SM, Hankenson KD. Wnt11 promotes osteoblast maturation and mineralization through R-spondin 2. J Biol Chem l2009;284: 14117-25.
[47] Felsher DW, Bishop JM. Reversible tumorigenesis by MYC in hematopoietic lineages. Mol Cell 1999;4: 199-207.
[48] Shimizu T, Ishikawa T, Sugihara E, Kuninaka S, Miyamoto T, Mabuchi Y, Matsuzaki Y, Tsunoda T, Miya F, Morioka H, Nakayama R, Kobayashi E, Toyama Y, Kawai A, Ichikawa H, Hasegawa T, Okada S, Ito T, Ikeda Y, Suda T, Saya H. c-MYC overexpression with loss of Ink4a/Arf transforms bone marrow stromal cells into osteosarcoma accompanied by loss of adipogenesis. Oncogene 2010;29: 5687-99.
[49] Hofbauer LC, Khosla S, Dunstan CR, Lacey DL, Boyle WJ, Riggs BL. The roles of osteoprotegerin and osteoprotegerin ligand in the paracrine regulation of bone resorption. J Bone Miner Res 2000;15: 2-12.
[50] Mogi M, Kondo A. The presence of TRAIL-OPG complex in human osteosarcoma and human salivary gland adenocarcinoma. J Immunoassay Immunochem 2011;32: 70-8.

Figure Legends

Figure 1. *In vivo* regulation of p53 in osteoblasts, Kaplan Meier survival graph and tumor pathology of *Osx*-Cre p53.1224 *pRb* animals. A-B) Schematic representation of the genetic strategy used to generate osteoblast restricted shRNA expression. **C**) Expression of endogenous p53 transcript in purified osteoblastic populations ($CD45^-CD31^-CD51^+$) from control (Osx-Cre+ p53.1224-ve; n= 4) and hairpin expressing animals (Osx-Cre+ve p53.1224+ve; = 3) at 4-8 weeks of age. Data expressed as mean ± SEM. **D**) Kaplan Meier survival plot of *Osx*-Cre+ve $p53^{fl/fl}$ *pRb* (red line, n=49) and *Osx*-Cre+ve p53.1224+ve *pRb* (black line, n=24). All Rb genotypes pooled. **E**) H&E stained section of primary Cre:lox OS and shRNA OS (all from independent animals). **F**) von Kossa stained section of primary and metastatic tumors from Cre:lox OS and shRNA OS as indicated. **G**) Liver metastasis of shRNA OS (white arrows). Enlarged view of liver metastasis demonstrating areas of mineralization. Scale bars as indicated on individual image.

Figure 2. MicroCT imaging and qPCR profiling of tumors. **A**) Representative μCT image of tibial tumors from Cre:lox (left) and shRNA (right) models. **B**) Mineral density analysis of a normal tibia and a tibial tumor derived from shRNA mouse. **C**) μCT guided pathology on a *Osx*-Cre+ve p53.1224+ve $pRb^{fl/+}$ animal that presented with paralysis. μCT imaging enabled identification of the tumor (white arrows). **D**) μCT imaging of metastatic disease. Note the heavily mineralized lung metastasis (white arrows) and primary lesion of the fore-limb (black arrow). **E**) μCT imaging of tumor progression *in vivo*. The initial tumor was identified on the upper fibula (single white arrow) and then 6 weeks later was seen to have progressed down the length of the fibula and begun to invade the tibia. **F**) Schematic of osteoblast lineage commitment. **G**) qPCR profiling of primary isolated WT osteoblasts ($lin^-CD45^-CD31^-Sca\text{-}1^{+/-}CD51^+$; n=4 independent isolations), Cre:lox whole tumors (n=7), shRNA primary whole tumors (n=8) and shRNA metastatic tumors (n=8) for the indicated genes. Also included are measurements of serum alkaline phosphatase from the peripheral blood at autopsy of control

(WT C57Bl6 males, age matched), shRNA OS bearing animals (n=4) and Cre:lox OS bearing animals (n=4). **H**) Serum alkaline phosphatase levels measured at autopsy in indicated cohorts. **I**) Ratio of cyclic AMP produced in response to stimulation by PTH (1-34) or isoproteronol in Cre:lox and shRNA OS early passage cell lines. All data expressed as mean ± SEM with Bonferroni correction for multiple comparisons.* $P<0.05$; ^{x} $P<0.01$.

Figure 3. Cell surface phenotype of OS. **A**) Cell surface profiling for Sca-1 and CD51 (αV Integrin) on early passage cell lines derived from Cre:lox and shRNA OS tumors. All populations were less than passage 5 and had less than 1% contamination with CD45+ve cells. Pre-osteoblasts have a surface phenotype of Sca-$1^{+}$$CD51^{+}$ and as they mature the cell phenotype becomes Sca-$1^{lo/-}$$CD51^{+}$. Quantitation of Sca-1/CD51 populations in the two models (n>3 per group). **B**) Expression of *Osx*-Cre:GFP compared to Sca-1. Quantitation of Sca-1/*Osx*-CreGFP populations in the two models (n>3 per group). **C**) Expression of PDGFRα (CD140a) compared to Sca-1 on Cre:lox and shRNA OS cell lines. Quantitation of Sca-1/PDGFRα populations in the two models (n>3 per group).

Figure 4. shRNA OS display a loss of function p53 pathway. **A**) Expression of endogenous p53 in cell lines; WT Ob n=4, Cre:lox OS n>3, shRNA OS primary n=14, shRNA met n=13. **B**) Induction of $p21^{Cip1}$ or Noxa in response to treatment with doxorubicin for 6hrs. **C**) Assessment of the affects of demethylation on p53 expression in control (Kusa4b10 cell line) and 3 shRNA OS cell lines following treatment for 3 days with azacytidine (AzadC), doxorubicin (6hrs), or both AzadC and doxorubicin (3 days AzadC with final 6hrs addition of doxorubicin). Upper panel shows endogenous p53 transcript expression relative to HPRT; lower panel the induction of Noxa in control (Kusa4b10), Cre:lox cell lines (n=3) and shRNA cell lines (n=3). Data are expressed as fold induction relative to HPRT levels; expressed as mean ± SEM with Bonferroni correction for multiple comparisons. *$P<0.05$.

Figure 5. Recurrent chromosomal changes in OS. **A**) Representative examples of M-FISH spectral karyotyping of two independently derived shRNA OS lines. **B**) Summary of chromosomal gains (grey bars) and losses (black bars). **C**) Summary of the chromosomal rearrangements for the six shRNA OS cell lines assessed.

Figure 6. Gene expression profiles of Cre:lox and shRNA OS. **A**) Heat map of the top 25 differentially expressed genes in each model between 4 Cre:lox OS primary tumors compared to 4 shRNA primary OS tumors respectively. Genes of interest displaying a 2-fold or greater change in expression and a $P<0.05$ in either model indicated. Examples of genes in selected pathways are provided. Total number of genes upregulated in each model indicated in box. **B**) Examples of gene set enrichment analysis (GSEA) pathways upregulated in Cre:lox OS compared to shRNA OS. **C**) Ingenuity Pathway Analysis of transcription factor programs significantly deregulated (z score ± 2.0, $P < 0.05$) between Cre:lox and shRNA OS. **D**) Metagene projection analysis of human and murine OS. Human sarcoma samples were used to define the metagene for each of 7 different human sarcomas (Training set; F7 defines the metagene for human osteosarcoma, # indicates osteosarcoma datasets independent of species). Murine sarcoma samples (all with an "m" preceding tumor type) were added as unknowns and classified according to the metagene derived from the training sets (Data from current study indicated in bold, mOS (Cre:lox) are samples from our previous study describing the *Osx*-Cre $p53^{fl/fl}$ $pRb^{fl/fl}$ model). Additional human test sarcoma sets were added to test the robustness of the metagene classification.

Figure 7. Proposed model of development of osteoblastic osteosarcoma using shRNA. A) Schematic of normal osteoblast maturation **B**) Cre:lox OS. Osteoblast differentiation is abruptly delayed at the pre-osteoblast stage of differentiation. This results in the development of a fibroblastic OS phenotype. **C**) shRNA OS. A gradual reduction of p53 as the osteoblasts mature results in an osteoblastic OS.

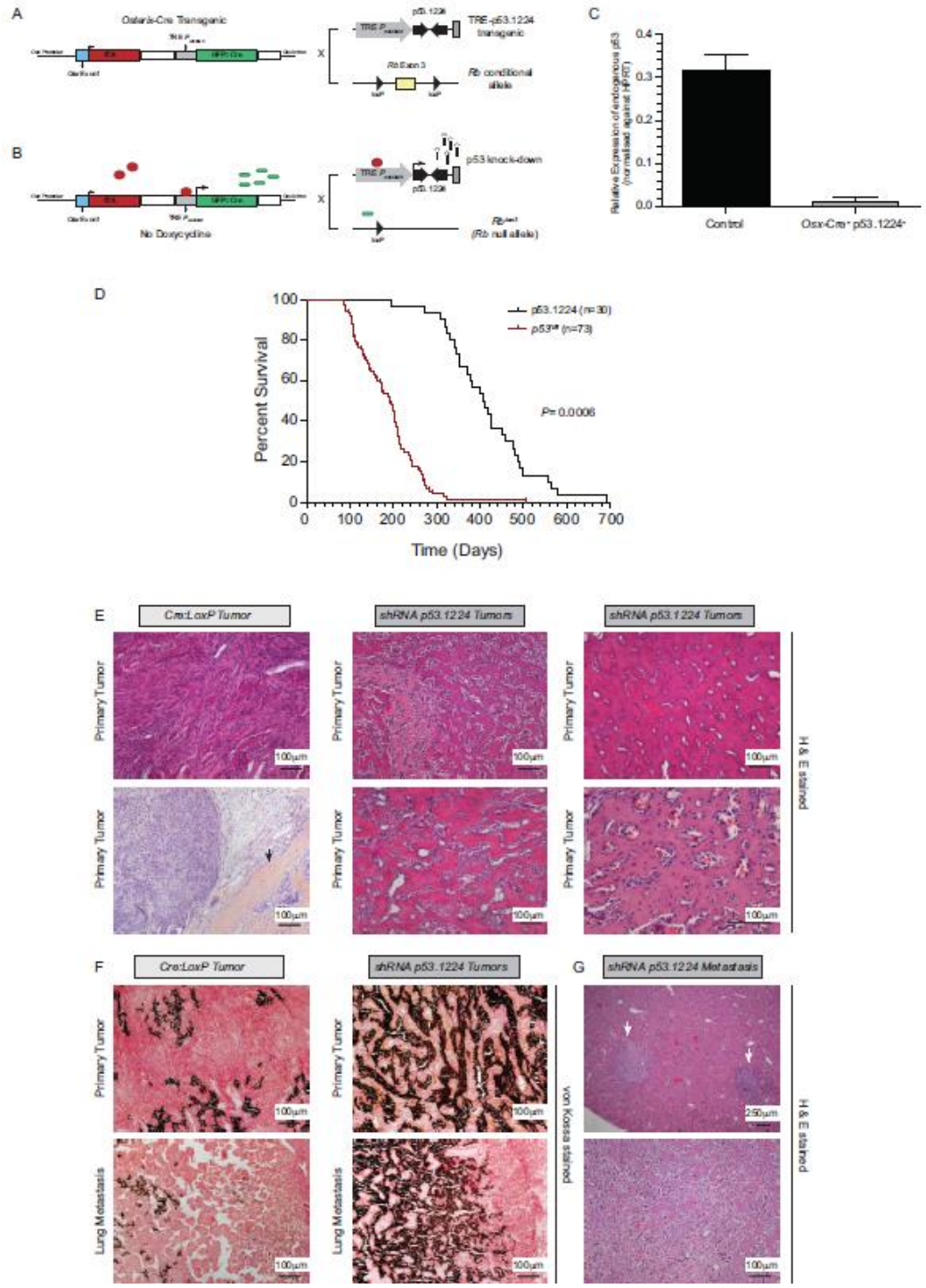

Figure 1

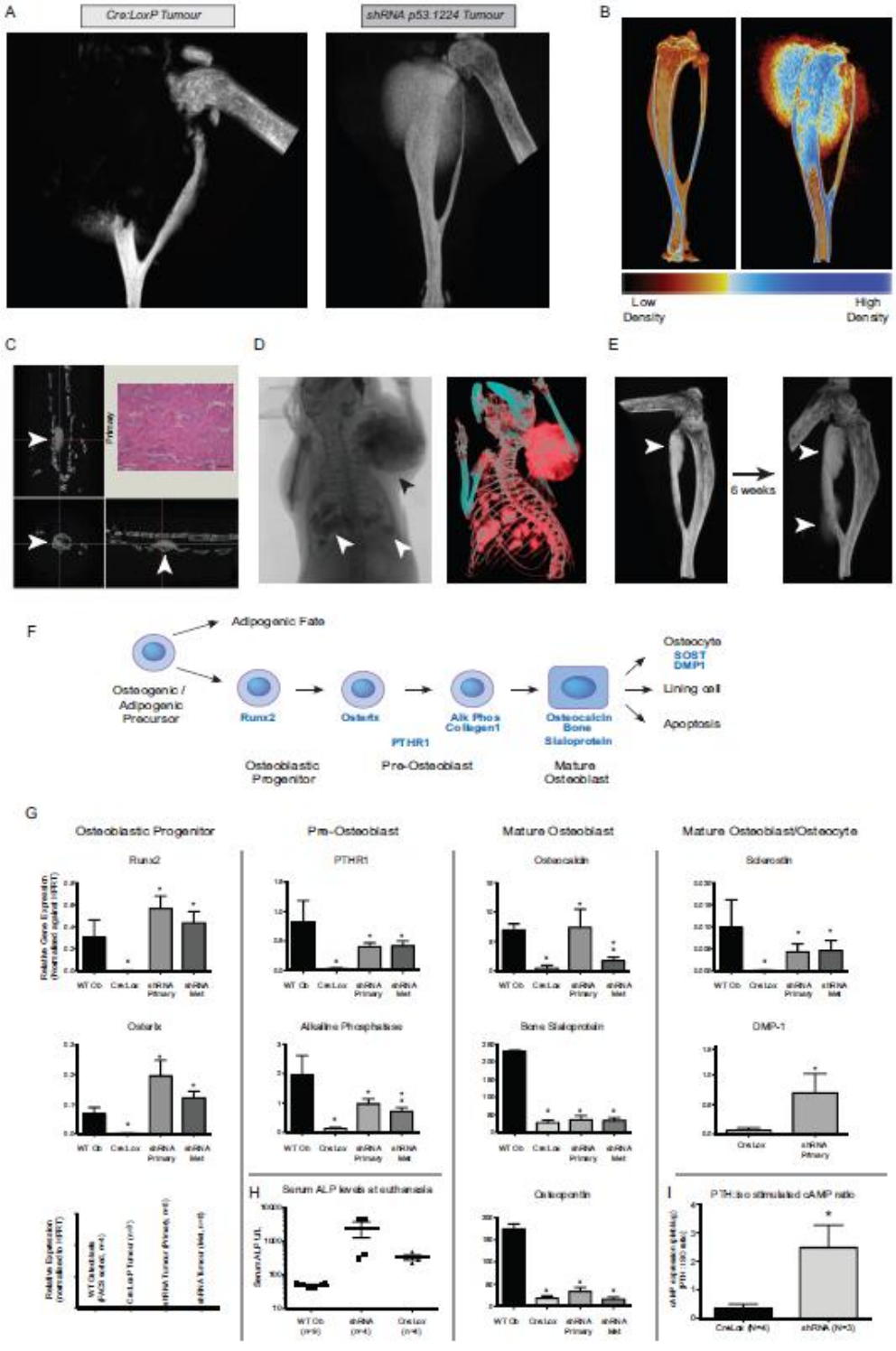
A
Cre:LoxP Tumour
shRNA p53.1224 Tumour
B
Low Density
High Density
C
D
E
6 weeks
F
Adipogenic Fate
Osteogenic / Adipogenic Precursor
Runx2
Osterix
Alk Phos
Collagen1
PTHR1
Osteocalcin
Bone Sialoprotein
Osteocyte
SOST
DMP1
Lining cell
Apoptosis
Osteoblastic Progenitor
Pre-Osteoblast
Mature Osteoblast
G
Osteoblastic Progenitor
Pre-Osteoblast
Mature Osteoblast
Mature Osteoblast/Osteocyte
Runx2
PTHR1
Osteocalcin
Sclerostin
Osterix
Alkaline Phosphatase
Bone Sialoprotein
DMP-1
H
Serum ALP levels at euthanasia
Osteopontin
I
PTH-stimulated cAMP ratio

Figure 2

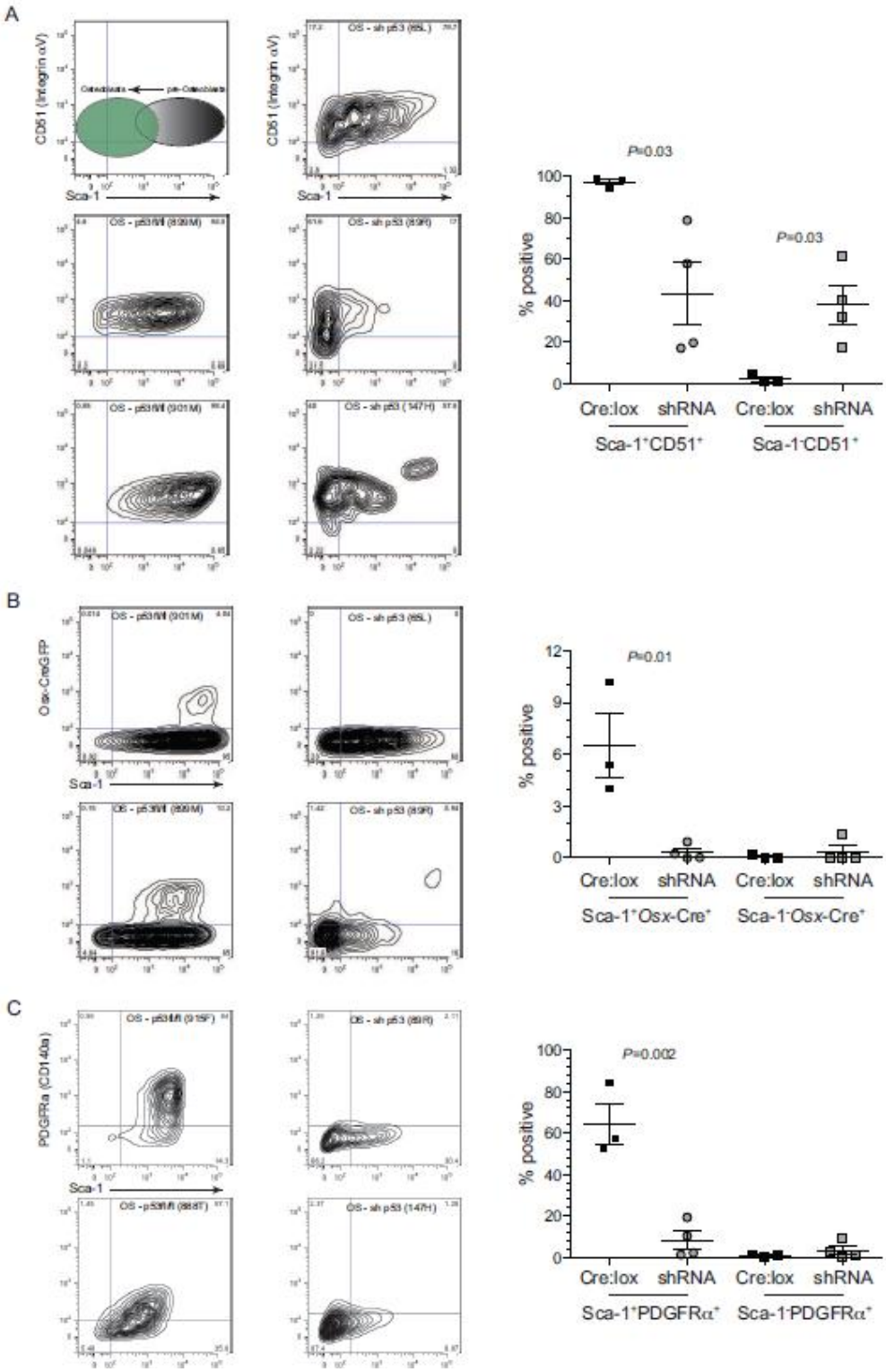
A
CD51 (Integrin αV)
Sca-1
Osteoblasts
pre-Osteoblasts
OS - sh p53 (85L)
OS - p53fl/fl (85IM)
OS - sh p53 (85H)
OS - p53fl/fl (91IM)
OS - sh p53 (147H)
P=0.03
P=0.03
% positive
100
80
60
40
20
0
Cre:lox
shRNA
Cre:lox
shRNA
Sca-1+CD51+
Sca-1-CD51+
B
Osx-CreGFP
Sca-1
OS - p53fl/fl (91IM)
OS - sh p53 (85L)
OS - p53fl/fl (85IM)
OS - sh p53 (85H)
P=0.01
% positive
12
9
6
3
0
Cre:lox
shRNA
Cre:lox
shRNA
Sca-1+Osx-Cre+
Sca-1-Osx-Cre+
C
PDGFRa (CD140a)
Sca-1
OS - p53fl/fl (91SF)
OS - sh p53 (85IR)
OS - p53fl/fl (85IT)
OS - sh p53 (147H)
P=0.002
% positive
100
80
60
40
20
0
Cre:lox
shRNA
Cre:lox
shRNA
Sca-1+PDGFRα+
Sca-1-PDGFRα+

Figure 3

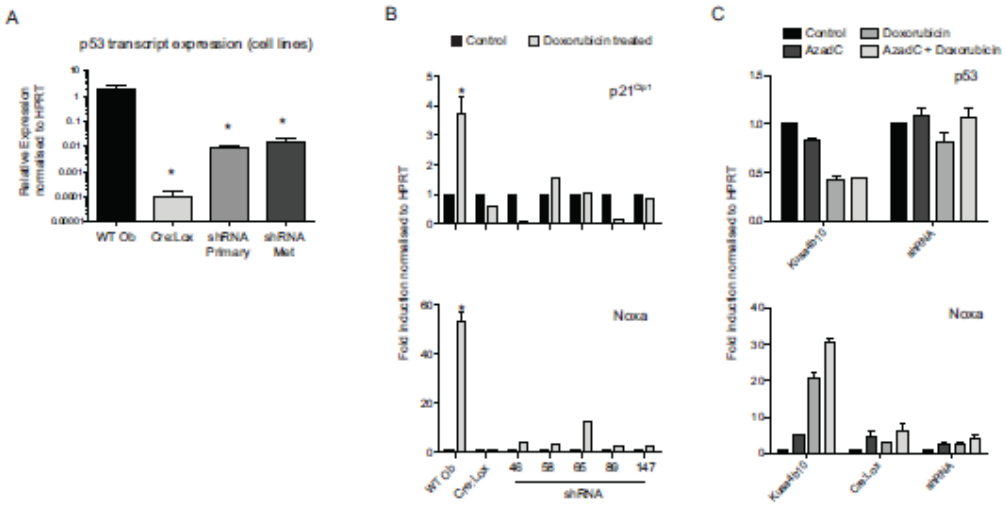

Figure 4

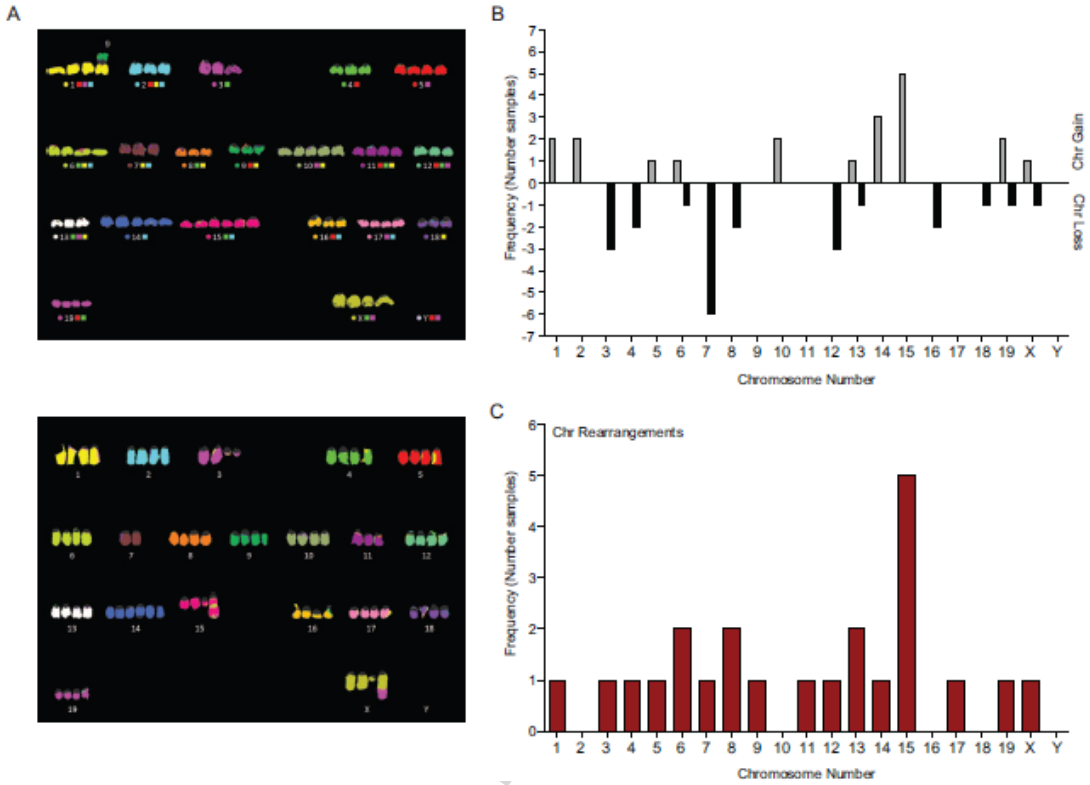

Figure 5

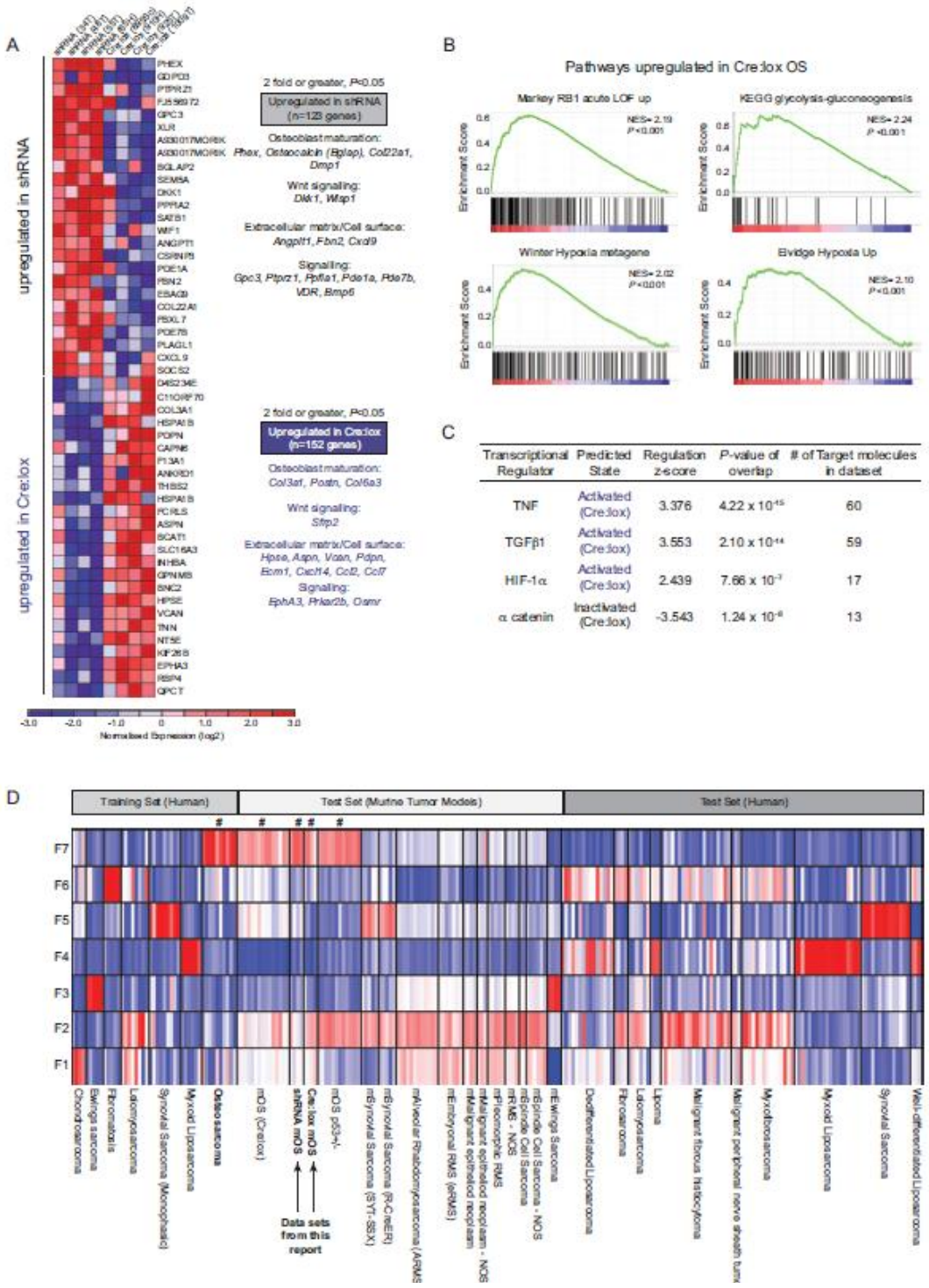

Transcriptional Regulator	Predicted State	Regulation z-score	P-value of overlap	# of Target molecules in dataset
TNF	Activated (Cre:lox)	3.376	4.22×10^{-15}	60
TGFβ1	Activated (Cre:lox)	3.553	2.10×10^{-14}	59
HIF-1α	Activated (Cre:lox)	2.439	7.66×10^{-7}	17
α catenin	Inactivated (Cre:lox)	-3.543	1.24×10^{-6}	13

Figure 6

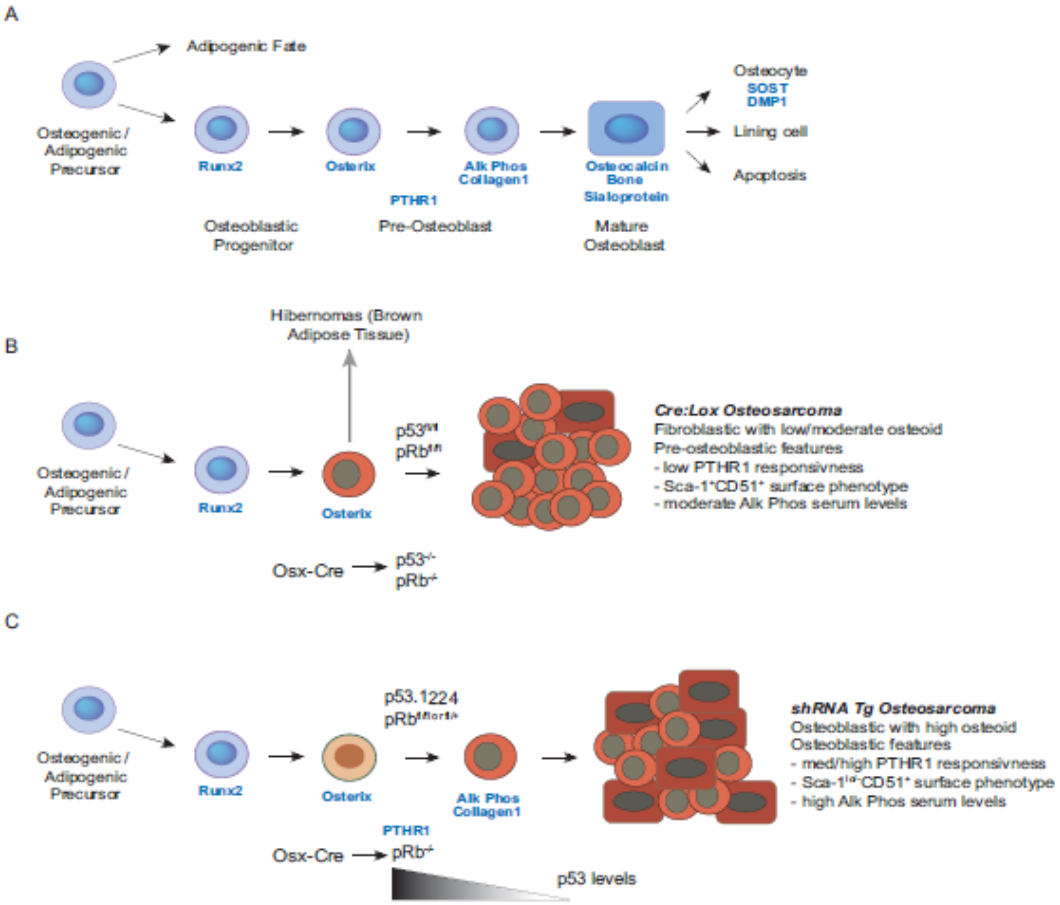

Figure 7

Highlights:

- Model of osteoblastic osteosarcoma
- Highly penatrent and metastatic disease
- Modeling of distinct tumor subtypes by shRNA compared to Cre:lox